Available online at www.sciencedirect.com
ScienceDirect
Journal of Power Sources 160 (2006) 57–64
JOURNAL OF POWER SOURCES
www.elsevier.com/locate/jpowsour

$Ba_{0.5}Sr_{0.5}Co_{0.8}Fe_{0.2}O_{3-\delta}$ as a cathode for IT-SOFCs with a GDC interlayer

Zaoshu Duan [a,b], Min Yang [a,b], Aiyu Yan [a,b], Zifang Hou [a], Yonglai Dong [a], You Chong [a], Mojie Cheng [a,*], Weishen Yang [a]

[a] *Dalian Institute of Chemical Physics, Chinese Academy of Sciences, Dalian 116023, China*
[b] *Graduate University of the Chinese Academy of Sciences, China*

Received 5 October 2005; received in revised form 27 December 2005; accepted 11 January 2006

Abstract

The chemical compatibility of the $Ba_{0.5}Sr_{0.5}Co_{0.8}Fe_{0.2}O_{3-\delta}$ (BSCF) with the yttria-stabilized zirconia (YSZ) electrolyte or Gd-doped ceria electrolyte (GDC), as well as that of the GDC with the YSZ electrolyte were examined. It was found that BSCF had a good compatibility with the GDC electrolyte but a poor chemical compatibility with the YSZ electrolyte. The BSCF cathode was adopted for anode-supported YSZ electrolyte cells with and without the application of a 1 μm thick GDC buffering layer between the cathode and the YSZ electrolyte. The interfacial reactions of the BSCF with the YSZ electrolyte surface and the GDC coated YSZ surfaces were investigated. The single cells were evaluated by using *I–V* curve measurements and AC impedance spectroscopy. The results depicted a great improvement in cell performance and a significant decrease in polarization resistance after adding the GDC buffer layer. The optimum firing temperature of the GDC film onto the YSZ film was around 1250 °C, which led to the maximum power density of 1.56 W cm^{-2} at 800 °C using air as oxidant and hydrogen as fuel.

Keywords: BSCF; Anode-supported solid oxide fuel cells; GDC interlayer; YSZ

1. Introduction

Solid oxide fuel cell (SOFC) has emerged as one of the most important power generation technologies because of its high-energy conversion efficiency, low noise and low pollution. For the traditional cell structures, the necessity for high operating temperatures (800–1000 °C) has resulted in high costs and material compatibility challenges [1]. As a consequence, significant effort has been devoted to the development of intermediate temperature solid oxide fuel cells (600–800 °C; IT-SOFCs). Among various cell structures, the anode-supported cell design with thin film of yttria-stabilized zirconia electrolyte (YSZ) has been extensively investigated in recent years because of its high power density and relatively low fabrication cost. Souza et al. reported that an anode-supported SOFC with an YSZ electrolyte film of ~10 μm, a Ni-YSZ anode and a $La_{1-x}Sr_xMnO_3$ (LSM)-based cathode could achieve a power density of 1.8 W cm^{-2} at 800 °C [2]. Wang et al. achieved a maximum power density as high as 2.24 W cm^{-2} at 800 °C under similar conditions [3]. On this type of cells, the cathode polarization resistance becomes the primary factor limiting cell performance in intermediate temperature range [2,4,5]. For the further improvement of cell performance, the development of higher performance cathode material is critical.

Mixed ionic and electronic conductors attract much attention as cathodes because they possess a triple-phase boundary region extending over the entire surface of the cathode, as O^{2-} ions produced on the surface of the cathode may be carried to the electrolyte by virtue of cathode ionic conduction pathways. Perovskite oxide $Ba_{0.5}Sr_{0.5}Co_{0.8}Fe_{0.2}O_{3-\delta}$ (BSCF) is a new mixed ionic and electronic conducting material with high catalytic activity and good oxygen permeability [6], and it shows an excellent performance as cathode on ceria electrolyte in low temperature range from 400 °C to 600 °C [7]. Known the high oxygen permeation flux above 650 °C [6], the BSCF would be an excellent cathode material using air as oxidant for IT-SOFC. However, most Co-containing cathode materials are chemically incompatible with the YSZ electrolyte. For

* Corresponding author. Tel.: +86 411 84379049; fax: +86 411 84379049.
E-mail address: mjcheng@dicp.ac.cn (M. Cheng).

0378-7753/$ – see front matter © 2006 Elsevier B.V. All rights reserved.
doi:10.1016/j.jpowsour.2006.01.092

example, the $La_{1-x}Sr_xCo_{1-y}Fe_yO_{3-\delta}$ (LSCF) cathode reacted readily with YSZ at high temperature, and the formation of high resistance phases deteriorated the cell performance [8,9]. Therefore, the Co-containing cathodes cannot be applied directly on the YSZ electrolyte. The materials chemically compatible with Co-containing cathodes are CeO_2 electrolytes [10,11], which possess a higher ionic conductivity than YSZ but cannot be used as electrolytes in intermediate temperature range because of their high electronic conductivity [12]. In order to use cobaltite perovskite type oxides as cathode material for IT-SOFCs, a thin film of Gd-doped ceria (GDC) has been proposed as a protective layer on the YSZ electrolyte [13–15]. But the solid-state reaction and interdiffusion phenomena between YSZ and GDC at high temperature will induce the formation of (Zr, Ce)O_2-based solid solutions which have a very low electrical conductivity [15–17]. Therefore, it is important to choose a proper firing temperature for the GDC layer to alleviate the unfavorable reaction between YSZ and GDC, and simultaneously to prevent the reaction between the cathode and YSZ.

In this study, the chemical compatibility of the BSCF with YSZ or GDC was tested and anode-supported SOFCs were fabricated with Ni-YSZ cermet, YSZ, BSCF and GDC used as anode, electrolyte, cathode and interlayer, respectively. Also the optimum firing temperature of GDC interlayer was investigated by using X-ray diffraction (XRD), cell performance and AC impedance measurements.

2. Experimental

The $Ba_{0.5}Sr_{0.5}Co_{0.8}Fe_{0.2}O_{3-\delta}$ (BSCF) and $Gd_{0.1}Ce_{0.9}O_{1.95}$ (GDC) powders were prepared by a combined citrate and EDTA complexing method [5]. The chemical compatibility of BSCF and YSZ (8 mol% Y_2O_3, from Tosoh Company) was examined by co-firing of the BSCF and YSZ powders at 800–1000 °C for 2 h in a 1:1 weight ratio. In addition, the chemical compatibility of BSCF with GDC was tested in the same way after co-firing at 950 °C for 2 h. XRD was used to determine the presence of any reaction products.

The green bodies of NiO-YSZ anode substrates were prepared from the mixed powders of nickel oxide (NiO, from J.T. Baker) and YSZ in a 6:4 weight ratio. The YSZ thin film was prepared onto the NiO-YSZ substrates by the tape-casting method and co-firing at 1400 °C. The thickness of YSZ film was about 15 μm. The GDC layer was coated with a GDC slurry onto the YSZ electrolyte, and fired at 1100–1400 °C for 1 h in air. The thickness of GDC film was about 1 μm by SEM analysis. The cathode was screen-printed on the YSZ or GDC film using the slurry of BSCF, and fired at 950 °C for 2 h. The effective area of the cathode was 0.5 cm^2, and the thickness was about 80–90 μm.

In order to investigate the interfacial reactions between BSCF and the YSZ electrolyte film and the GDC coated YSZ electrolyte films, the BSCF cathodes after fired at 950 °C and 1050 °C for 2 h were scrapped off the cells. XRD patterns were taken on the electrolyte surface to detect the interfacial reaction products.

The single cells were sealed on one end of alumina tube. Silver meshes were used as current collectors and spring-pressed against the anode and cathode. After the in situ reduction of the NiO anode in H_2 for several hours, the performances of the cell were measured at 650–800 °C by changing an external load. The *I–V* characteristic of the anode-supported cell was measured using humidified hydrogen as the fuel (70 ml min^{-1}) and air as the oxidant (200 ml min^{-1}). The impedances were measured typically under open circuit conditions using a Solartron 1287 potentiostat and 1260 frequency response analyzer with a computer. The frequency range was from 0.01 Hz to 10 kHz with signal amplitude of 10 mV.

3. Results and discussion

3.1. Chemical compatibility of BSCF with YSZ or GDC

Fig. 1 shows the XRD patterns of the fired mixtures of BSCF and YSZ. The diffraction pattern of BSCF powder is also shown as a reference. After fired at 800 °C and 850 °C, the mixed power depicts the diffraction peaks only from BSCF and YSZ. This means that the two materials have a good chemical compatibility at low temperatures. However, the cathode is required to be fired onto the electrolyte at least at above 900 °C. At a firing temperature of 900 °C, some new diffraction peaks appear in these diffraction patterns, which can be attributed to $BaZrO_3$. The diffractions for $BaZrO_3$ gradually increase in intensities with firing temperature. After fired at 950 °C, the diffraction peaks for BSCF completely disappear, and some new diffraction peaks, which can be ascribed to Co_3O_4 and $Sr_2(CoFe)O_5$, appear. So, BSCF has poor chemical compatibility with YSZ, and it could not directly be applied as cathode on the YSZ electrolyte.

Fig. 2 shows the XRD patterns of several mixed powders. When the mixture of BSCF and GDC was fired at 950 °C for 2 h in air, no new reaction product was detected, revealing that BSCF cathode has a good chemical compatibility with the GDC electrolyte. Since the GDC interlayer can react with the YSZ electrolyte at higher temperature, it is necessary to learn the chemical compatibility of the BSCF with the solid solution of

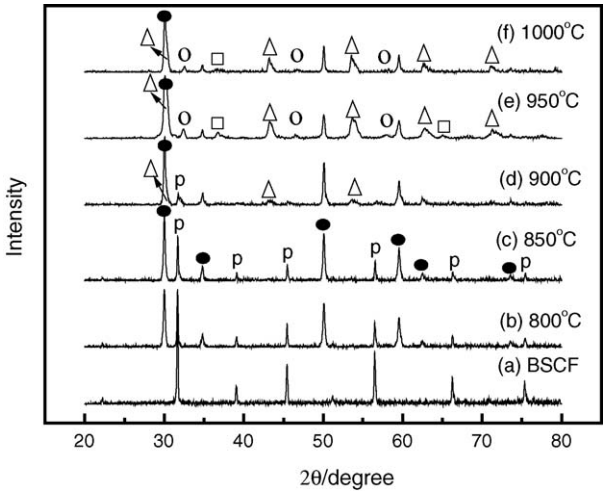

Fig. 1. XRD patterns of (a) BSCF and the mixtures of BSCF and YSZ fired at (b) 800 °C, (c) 850 °C, (d) 900 °C, (e) 950 °C and (f) 1000 °C. (●) YSZ, (p) BSCF, (△) $BaZrO_3$, (□) Co_3O_4 and (◯) $Sr_2(FeCo)O_5$.

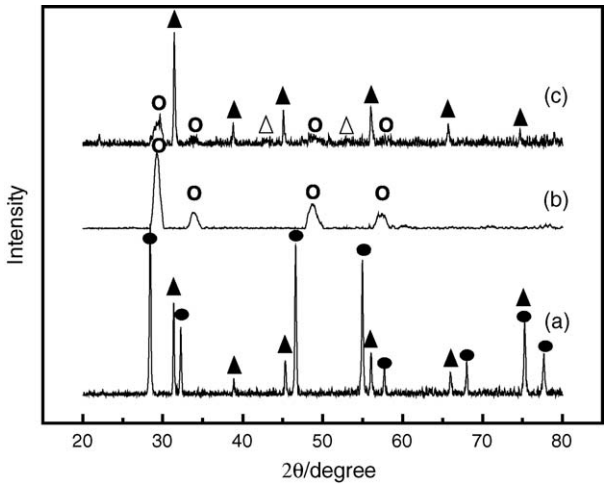

Fig. 2. XRD patterns of (a) the mixture of BSCF and GDC fired at 950 °C for 2 h, (b) the mixture of YSZ and GDC with 1:1 weight ratio fired at 1400 °C for 1 h and (c) the mixture of BSCF and solid solution GDC-YSZ fired at 950 °C for 2 h. (●) GDC, (▲) BSCF, (◯) solid solution of GDC-YSZ and (△) $BaZrO_3$.

GDC-YSZ. A single phase of solid solution GDC-YSZ was gotten through firing the mixture of YSZ and GDC at 1400 °C for 1 h, as shown in Fig. 2. When the solid solution of GDC-YSZ and BSCF were mixed and fired at 950 °C for 2 h in air, the diffraction patterns mainly consist of the two phases from BSCF and the solid solution. In the meantime, some new phases, which may be ascribed to $BaZrO_3$, also appear. The low reactivity of the solid solution of GDC-YSZ with BSCF at 950 °C can either be due to the doping of Ce^{4+} in YSZ and/or the large particle size of the solid solution. Thus, the choice for adopting BSCF cathode onto the YSZ electrolyte is to add a dense interlayer of pure GDC with an appropriate firing temperature.

3.2. Thin GDC layer to buffer the interfacial reactions

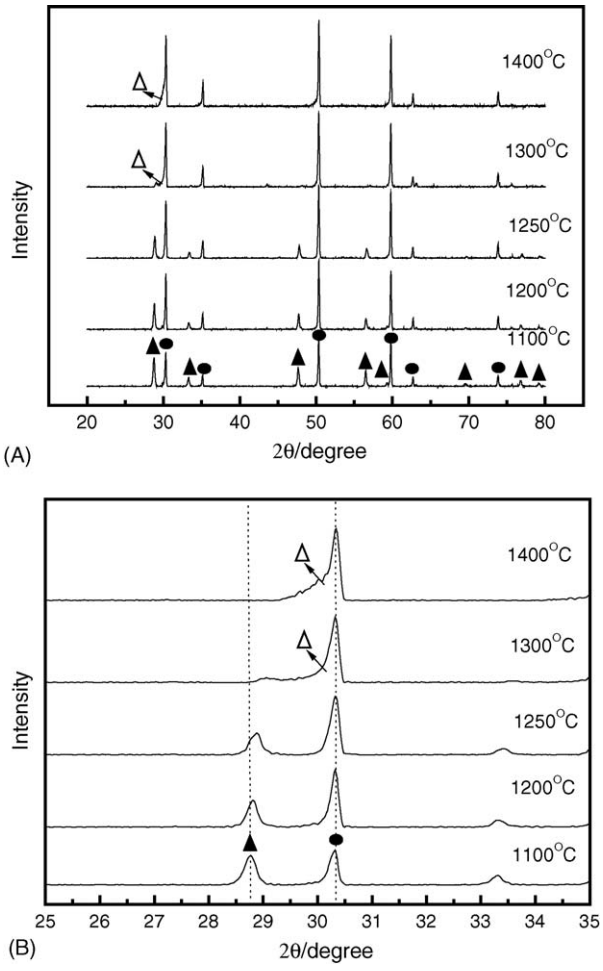

Fig. 3. XRD patterns of the anode–electrolyte assemblies with the GDC layer fired on the YSZ film at different temperatures. The patterns were taken from the GDC layer side. (▲) GDC, (●) YSZ and (△) (Zr, Ce)O_2 solid solution.

Fig. 3A shows XRD patterns of the anode supported electrolyte assemblies with the GDC layer fired on the YSZ film at different temperatures. The patterns were taken from the GDC layer sides. Since the GDC films are very thin, typically about 1 μm, both the diffraction patterns of GDC and YSZ can be observed in Fig. 3A. The changes of diffraction peaks of GDC and YSZ after the interfacial reactions or interdiffusion are well depicted in these patterns. After fired at 1100 °C, the diffraction pattern consists of the two cubic fluorite phases of GDC and YSZ, and there are no secondary phases present. With the increase of the firing temperature, the diffraction peaks for GDC become weak and those for YSZ become strong, suggesting the decrease in the thickness of the GDC layer. Moreover, the peaks of GDC gradually shift to higher angles than the origin position at 1100 °C and 1200 °C, which results from the diffusion of small cations of Zr^{4+} and/or Y^{3+} into the GDC lattice [16,18–20]. The phenomenon is more clearly observed in Fig. 3B, which magnifies the diffraction peaks. In the meantime, each YSZ diffraction peak grows a tail at the low angle side, suggesting that some Ce^{4+} and/or Gd^{3+} cations diffused into the YSZ layer and formed a GDC-YSZ solid solution at the interface. The main diffraction angles of YSZ remain unchanged, which reflects the reaction occurred only at the interfaces of the GDC film and the dense YSZ film. The solid solutions ZrO_2–$YO_{1.5}$–CeO_2–$GdO_{1.5}$ are formed at the GDC/YSZ interface at above 1200 °C. The diffraction peaks for GDC from the cubic ceria phase become very weak after firing at 1300 °C, and disappear at 1400 °C, suggesting a complete solid-state reaction of GDC with YSZ to form the solid solution. The sharp diffraction peaks from YSZ and the grown-up tails at the low angle sides indicate that the GDC film was converted into a solid solution of ZrO_2–$YO_{1.5}$–CeO_2–$GdO_{1.5}$. Formations of (Zr, Ce)O_2-based solid solutions are not desirable because such solid solutions exhibit much lower ionic conductivities than GDC and YSZ and may lower cell performance and a poor chemical compatibility with the BSCF cathode material.

Fig. 4 shows SEM photograph of GDC surface of BSCF/GDC/YSZ/Ni-YSZ with the GDC layer fired at 1100–1400 °C and cross-section of BSCF/GDC/YSZ/Ni-YSZ with the GDC layer fired at 1250 °C. With the increase of firing temperature, GDC particles were sintered into larger ones. Since the GDC films were deposited on the sintered anode-supported YSZ films, only the GDC particles could shrink during firing. Therefore, some pores were left on the surface of the GDC films. These pores were also enlarged with the increase of fir-

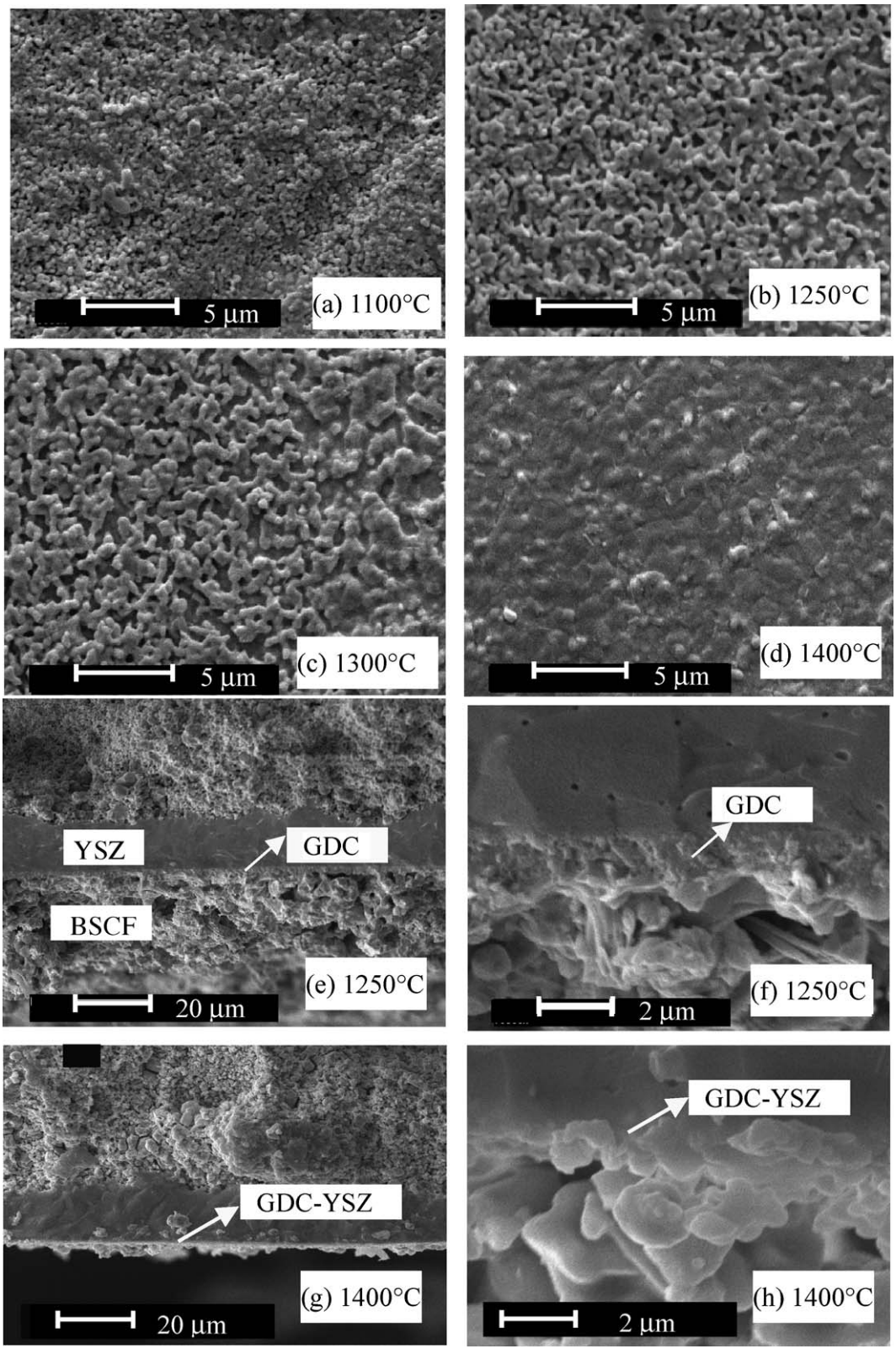

Fig. 4. SEM photograph of GDC surface of BSCF/GDC/YSZ/Ni-YSZ with the GDC layer fired at (a) 1100 °C, (b) 1250 °C, (c) 1300 °C, (d) 1400 °C, and the cross-section of BSCF/GDC/YSZ/Ni-YSZ with the GDC layer fired at (e, f) 1250 °C and (g, h) 1400 °C.

ing temperature. Though pores are present on the surface layer, the cross-section view depicts that the GDC layer near to the YSZ film is almost in a dense structure. When the GDC layer was fired at 1400 °C, the surface was dense and the pores disappeared, since the GDC layer is completely converted into the solid solution.

When the GDC layer is fired at 1250 °C, the buffering layer of GDC is ca. 1 μm and the thickness of the YSZ electrolyte

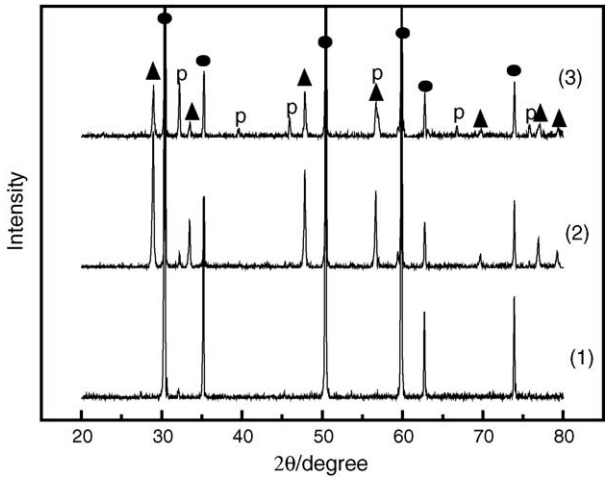

Fig. 5. XRD patterns of (1) BSCF/YSZ/Ni-YSZ and BSCF/GDC/YSZ/Ni-YSZ cell with GDC layer fired at (2) 1100 °C and (3) 1250 °C when the firing temperature of BSCF is 950 °C. The BSCF cathodes were scraped and the patterns were taken from the cathode side. (▲) GDC, (●) YSZ and (p) BSCF.

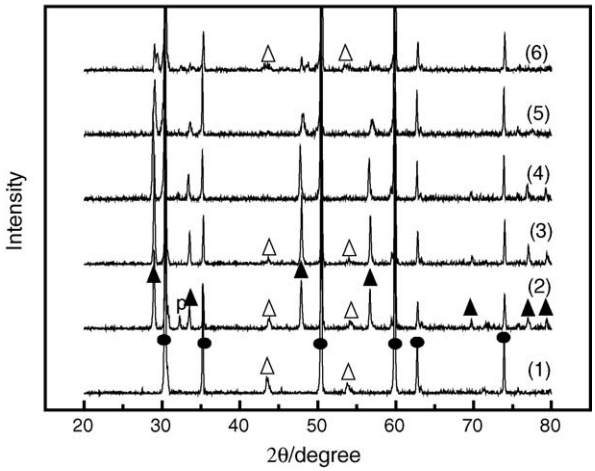

Fig. 6. XRD patterns of (1) BSCF/YSZ/Ni-YSZ and BSCF/GDC/YSZ/Ni-YSZ cell with GDC layer fired at (2) 1100 °C, (3) 1200 °C, (4) 1250 °C, (5) 1300 °C and (6) 1400 °C when the firing temperature of BSCF is 1050 °C. The BSCF cathodes were scraped and the patterns were taken from the cathode side. (▲) GDC, (●) YSZ, (p) BSCF and (□) $BaZrO_3$.

is 15 μm. The GDC film is successfully prepared on YSZ film. Cracks are not found on the GDC film. The GDC layer here is controlled as thin as possible by the slurry-coating method to improve the interfacial properties of electrode and the YSZ electrolyte. If the reactions between YSZ and BSCF can be well blocked with a dense sub-layer, a porous surface structure can enlarge three-phase boundary and may be good for suppressing the cathode–electrolyte interfacial resistance. However, the interlayer can be found in the cross-section pictures of the cell when the GDC layer was fired at 1400 °C. This is in good agreement with the serious reaction between GDC and YSZ depicted with the XRD result.

Fig. 5 shows the XRD patterns of the electrolyte surfaces of the BSCF/YSZ/Ni-YSZ cell and the BSCF/GDC/YSZ/Ni-YSZ cells with BSCF fired at 950 °C. In order to increase the sensitivity for detecting interfacial minor phases, these patterns were taken after the BSCF cathodes were scraped off. At 950 °C, no reaction product can be detected because the interfacial reaction is not severe at this temperature, and the reaction product of BSCF and YSZ is far less than the detection limit. So, the results do not indicate no reactions occurred between YSZ and BSCF.

In order to discriminate the role and difference of the buffer layers fired at different temperatures, the firing temperature of the BSCF cathode was increased to 1050 °C. Fig. 6 shows the XRD patterns of the BSCF/YSZ/Ni-YSZ cell and the BSCF/GDC/YSZ/Ni-YSZ cells with a firing temperature of BSCF of 1050 °C. The patterns were also taken on the electrolyte surfaces after the BSCF cathodes were scraped off. Because this series of cells were fabricated in different batch only for the XRD study, the GDC layer was not controlled as well as the previous series. The stronger peaks of GDC than those in Fig. 3 suggest that the GDC layer is thicker than that of the cells in Fig. 3. So in the pattern (6), two series of peaks can be related to the GDC layer, one for pure GDC and another for the GDC reacted with zirconia. The strange shifts of all the peaks in the pattern (4) to lower diffraction angles may be due to some technical reason with this XRD measurement. When BSCF is directly fired onto YSZ without GDC, some new diffraction peaks appear in these diffraction patterns, which can be attributed to $BaZrO_3$. The high resistance phase of $BaZrO_3$ is detected at the interfaces of BSCF and YSZ with the GDC layer fired at 1100 °C and 1200 °C, which means these GDC layers could not prevent the reactions between BSCF and YSZ. In this case, the reactions most probably occurred from the diffusion of Ba cations from cathode through the porous GDC layer to the YSZ surface. The diffractions for $BaZrO_3$ gradually decrease in intensities with the firing temperature increasing. With the GDC layer fired at 1250 °C, there are no new phases formed, and the GDC film successfully prevented the reactions between BSCF and YSZ. With the firing temperature of the GDC layer further increasing, the peaks from $BaZrO_3$ appear again. The intensities of the new peaks are very weak at 1300 °C and become stronger at 1400 °C. The formation of the high resistance phases is due to the reactions of BSCF and the solid solution GDC-YSZ when the GDC layer was fired at 1300 °C and 1400 °C. Therefore, the optimum firing temperature of the GDC layer is around 1250 °C.

3.3. Cell performance

Fig. 7 shows *I–V* and *I–P* curves of the BSCF/GDC/YSZ/Ni-YSZ cells and the BSCF/YSZ/Ni-YSZ cell. All the cells exhibit a decrease in performance with decreasing operating temperature due to the increase of the ohmic resistance and the polarization resistance. For the BSCF/YSZ/Ni-YSZ cell, the maximum power density (MPD) is just 0.44 W cm^{-2} at 800 °C. After adding the GDC layer, the cell performances show significant improvements. Since all the anode supported YSZ electrolyte bilayer assemblies were prepared in the same batch, the different power-generating characteristics of the cells mainly arise from the firing temperatures of the GDC layer, which determines the interfacial property of the cathode and the YSZ.

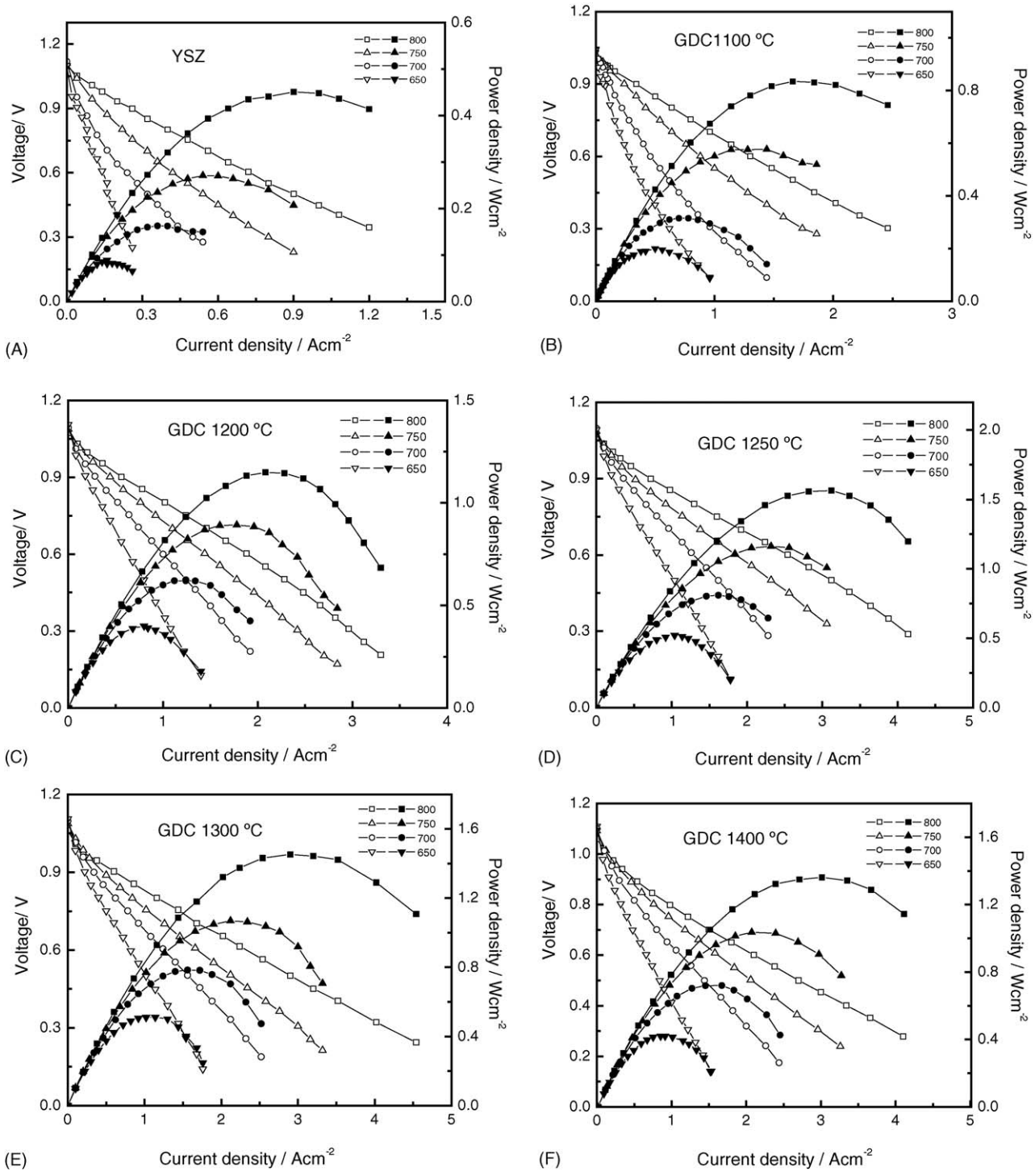

Fig. 7. *I–V* and *I–P* curves of (A) the BSCF/YSZ/Ni-YSZ cell and the BSCF/GDC/YSZ/Ni-YSZ cells with the GDC layer fired at (B) 1100 °C, (C) 1200 °C, (D) 1250 °C, (E) 1300 °C and (F) 1400 °C. The cells were operated using hydrogen as fuel and air as oxidant at different temperatures.

When the GDC layer is fired at 1250 °C, the highest performance is achieved, and the MPDs of the cell are 1.56 W cm^{-2}, 1.16 W cm^{-2}, 0.81 W cm^{-2} and 0.52 W cm^{-2} at 800 °C, 750 °C, 700 °C and 650 °C, respectively. The performance is comparable with that of the state-of-art cell with an LSM-YSZ cathode using oxygen as the oxidant [2,4,5]. The open circuit potential (OCP) is ca. 1.074 V at 800 °C, ca. 1.092 V at 650 °C, which are in good agreement with theoretical values.

The cell performances show parabolic dependence on the firing temperatures of the GDC layer. With firing temperature increase, the cell performance increases up to a maximum value then it decreases. Based on the cell performance, the best firing temperature of the GDC layer is 1250 °C, which is consistent with the interfacial reaction results. The increase of the performance with the firing temperature is attributed to an improvement in both connection among GDC grains and adhe-

sion in GDC/YSZ interface and a reduction in the detrimental reaction between BSCF and YSZ. With the temperature further increase, the performance slightly decreases, which results from the formation of the solid solution YSZ-GDC and the reaction between BSCF and the solid solution. It has been pointed out that the formation of the solid solution YSZ-GDC causes a deterioration of the electrolyte performance [15,17,21]. The results are consistent with the XRD of the BSCF/GDC/YSZ/Ni-YSZ systems in Fig. 6, which shows the GDC layer succeeded in preventing the reaction between BSCF and YSZ at 1250 °C. With the firing temperature increasing from 1250 °C to 1400 °C, the MPD decreases from 1.56 W cm^{-2} to 1.36 W cm^{-2} at 800 °C, which indicates the bad effect on cell performance is not serious. Though the cells with the GDC layer fired at 1400 °C or below 1200 °C also show a much better cell performance than the cell without GDC layer, the high chemical activity of BSCF with zirconia, as indicated in Fig. 6, cannot assure their long-term stability. The high performance of the cell with GDC layer fired at 1250 °C as well as the previous results indicate that the GDC interlayer sintered at 1250 °C is acting as an effective barrier to prevent reaction between the cathode and the YSZ electrolyte, while the BSCF cathode retains good performance on GDC in the intermediate temperature range.

3.4. Impedance analysis

Fig. 8 shows the impedance plot of the cell BSCF/YSZ/Ni-YSZ and those of the cells BSCF/GDC/YSZ/Ni-YSZ with the GDC layer fired at 1100–1400 °C. The impedance plots were measured at 800 °C under open circuit potential conditions using hydrogen as fuel and air as oxidant. The impedance of the BSCF/YSZ/Ni-YSZ cell are mainly determined by the character of the new phases formed at the interface of BSCF and YSZ because the conductivities of the new phases are extremely low. The polarization resistance of the BSCF/YSZ/Ni-YSZ cell is very large, which can reach 1.20 Ω cm^2 at 800 °C, while the ohmic resistance is just 0.19 Ω cm^2. The polarization resistance mainly comes from the cathode process in the anode-supported fuel cell [2,4,5]. The spectra can be characterized by a larger arc at high frequencies and a much smaller one at low frequencies. The high-frequency arc can be attributed to the charge transfer process on the cathode, which is contributed by the surface contact of the cathode particles on the electrolyte surface [22–24]. On the other hand, the low-frequency arc can be attributed to the gas diffusion of cathode [25]. The high polarization resistance results from the large amounts of new phases at the interface of BSCF and YSZ, which obstruct the contact of the cathode and the electrolyte and bring out a drastic decrease of the triple-phase region. The ohmic resistance is related to the total conductivities and mainly comes from the YSZ electrolyte film and the interface of cathode and electrolyte. The ohmic resistance is not high, which may be from the presence of silver from the current collecting layer and the good electronic conductivity phase $Sr_2(CoFe)O_5$ [26]. When fired onto a GDC film at 1100 °C, the polarization resistance slightly decreases, and the ohmic resistance remains similar to the cell without GDC layer. With the firing temperature increasing from 1100 °C to 1200 °C, the polarization resistance abruptly decreases from 0.81 Ω cm^2 to 0.28 Ω cm^2, and the ohmic resistance decreases from 0.19 Ω cm^2 to 0.165 Ω cm^2. At above 1200 °C (including 1200 °C), the variations of the polarization are very small. This suggests the new

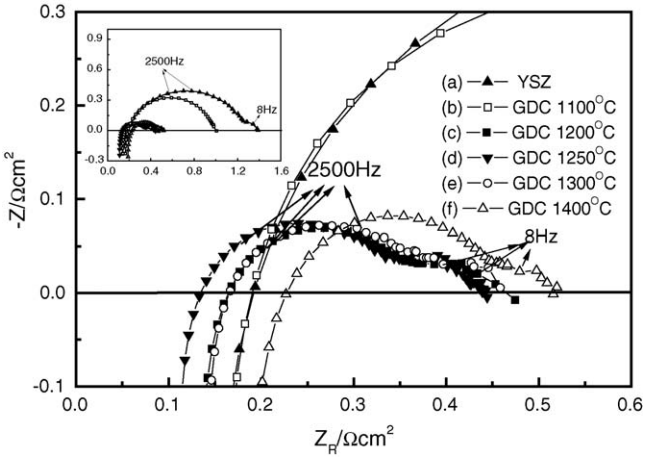

Fig. 8. Impedance plots of (a) the BSCF/YSZ/Ni-YSZ cell (YSZ) and the BSCF/GDC/YSZ/Ni-YSZ cells with the GDC layer sintered at (b) 1100 °C, (c) 1200 °C, (d) 1250 °C, (e) 1300 °C and (f) 1400 °C. The impedance plots were measured at 800 °C under open circuit potential conditions using hydrogen as fuel and air as oxidant.

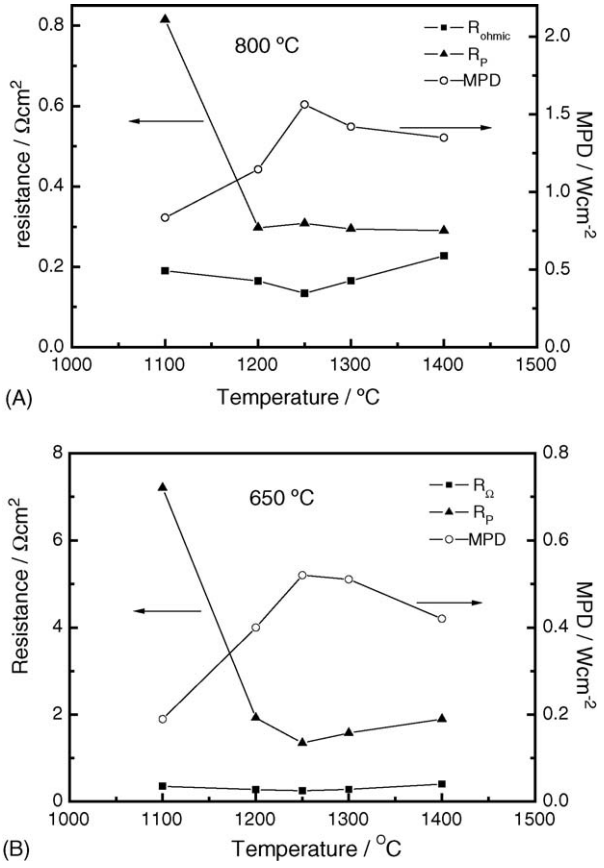

Fig. 9. Effect of the firing temperature of GDC layer on the maximum power density (MPD), ohmic resistance (R_{ohmic}) and polarization resistance (R_P) at (A) 800 °C and (B) 650 °C.

phases almost do not affect the triple-phase region. In the meantime, the spectra can be characterized by a larger arc at high frequencies and a much smaller one at low frequencies. The high-frequency arc can be attributed to the charge transfer process on the cathode, which may be due to large particle radius of the cathode. With firing temperature increasing, the ohmic resistance decreases to a minimum value of 0.135 $\Omega\,cm^2$ at 1250 °C, which is attributed to an improvement in both connection among GDC grains and adhesion in GDC/YSZ interface and a reduction in the detrimental reaction between BSCF and YSZ. With a further increase of firing temperature of GDC, the ohmic resistance slightly increases, which results from the formation of the solid solution YSZ-GDC and the reaction between BSCF and the solid solution above 1250 °C. Thus, the impedance results also depict that 1250 °C is the optimum firing temperature of the GDC film on the YSZ electrolyte because the total resistance including ohmic and politicization resistance is the smallest. The results are consistent with those of XRD analysis of GDC/YSZ interface and power output.

The ohmic resistance (R_Ω), the polarization resistance (R_P) and the maximum power density at 800 °C and 650 °C, respectively, as a function of the firing temperature of GDC layer are shown in Fig. 9. R_Ω and R_P are determined from the impedance spectra of the cells. When the firing temperature of GDC layer is 1250 °C, the ohmic resistance is smallest no matter the operating temperature is 800 °C or 650 °C. It is also clear that both the R_Ω and R_P affect the cell performance at 800 °C. However, the cell performance is essentially dominated by the R_P at 650 °C. When the firing temperature of GDC layer is 1250 °C, the R_P is 0.308 $\Omega\,cm^2$, one time higher than the R_Ω (0.135 $\Omega\,cm^2$) at 800 °C, and the former increased to 1.35 $\Omega\,cm^2$ at 650 °C, about five times of the value of the R_Ω (0.248 $\Omega\,cm^2$).

4. Conclusions

The reaction between BSCF and YSZ occurred at 900 °C and some new phases were formed, while BSCF has a good chemical compatibility with GDC. The solid-state reaction between YSZ and GDC is remarkable at 1300 °C. After introducing a 1 μm thick GDC film between the BSCF cathode and the YSZ electrolyte, the cell performances show large improvements along with a large decrease of polarization resistances. The cell performances show parabolic dependence on the firing temperatures of the GDC layer. The increase of the performance with the firing temperature is attributed to an improvement in both connection among GDC grains and adhesion in GDC/YSZ interface and a reduction in the detrimental reaction between BSCF and YSZ. With the temperature further increase, the performance slightly decreases, which results from the formation of the solid solution YSZ-GDC and the reaction between BSCF and the solid solution. The thin GDC interlayer successfully prevents unfavorable solid-state reactions between BSCF and YSZ. The optimum firing temperature of GDC film on YSZ electrolyte is around 1250 °C. The maximum power density with BSCF as cathode is 1.56 $W\,cm^{-2}$ using air as oxidant and hydrogen as fuel at 800 °C.

Acknowledgements

The authors gratefully acknowledge the financial supports from the Ministry of Science and Technology of China (Grant Nos. 2004CB719506 and 2005CB221404).

References

[1] N.P. Brandon, S. Skinner, B.C.H. Steele, Annu. Rev. Mater. Res. 33 (2003) 183.
[2] S.D. Souza, S.J. Visco, L.C. De Jonghe, J. Electrochem. Soc. 144 (1997) L35.
[3] Z.W. Wang, M.J. Cheng, Y.L. Dong, M. Zhang, H.M. Zhang, Solid State Ionics, Corrected Proof, available online 6 September 2005, in press.
[4] J.W. Kim, A.V. Virkar, K.Z. Fung, K. Mehta, S.C. Singhal, J. Electrochem. Soc. 146 (1999) 69.
[5] Y. Jiang, A.V. Virkar, F. Zhao, J. Electrochem. Soc. 148 (2001) A1091.
[6] Z.P. Shao, W.S. Yang, Y. Cong, H. Dong, G.X. Xiong, J. Membr. Sci. 172 (2000) 177.
[7] Z.P. Shao, S.M. Halle, Nature 431 (2004) 170.
[8] H.Y. Tu, Y. Takeda, N. Imanishi, O. Yamamoto, Solid State Ionics 117 (1999) 277.
[9] O. Yamamoto, Y. Takeda, R. Kanno, M. Noda, Solid State Ionics 22 (1987) 241.
[10] W.X. Chen, T.L. Wen, H.W. Nie, R. Zheng, Mater. Res. Bull. 38 (2003) 1319.
[11] L. Qiu, T. Ichikawa, A. Hirano, N. Imanishi, Y. Takeda, Solid State Ionics 158 (2003) 55.
[12] K. Eguchi, T. Setoguchi, T. Inoue, H. Arai, Solid State Ionics 52 (1992) 165.
[13] S. Charojrochkul, K.L. Choy, B.C.H. Steele, Solid State Ionics 121 (1999) 107.
[14] C. Rossignol, J.M. Ralph, J.-M. Bae, J.T. Vaughey, Solid State Ionics 175 (2004) 59.
[15] A. Tsoga, A. Gupta, A. Naoumidis, P. Nikolopoulos, Acta Mater. 48 (2000) 4709.
[16] T.L. Nguyen, K. Kobayashi, T. Honda, Y. Iimura, Solid State Ionics 174 (2004) 163.
[17] A. Tsoga, A. Naoumidis, D. Stover, Solid State Ionics 135 (2000) 403.
[18] N. Sakai, T. Hashimoto, T. Katsube, et al., Solid State Ionics 143 (2001) 151.
[19] H. Mitsuyasu, Y. Nonaka, K. Eguchi, Solid State Ionics 113–115 (1998) 279.
[20] H. Mitsuyasu, Y. Nonaka, K. Eguchi, H. Aral, J. Solid State Chem. 129 (1997) 74.
[21] A. Tsoga, A. Naoumidis, W. Jungen, D. Stfver, J. Eur. Ceram. Soc. 19 (1999) 907.
[22] F.H. van Heuveln, H.J.M. Bouwmeester, J. Electrochem. Soc. 144 (1997) 134.
[23] Y.J. Leng, S.H. Chan, K.A. Khor, S.P. Jiang, Int. J. Hydrogen Energy 29 (2004) 1025.
[24] H.-C. Yu, F. Zhao, A.V. Virkar, K.-Z. Fung, Electrochemical characterization and performance evaluation of intermediate temperature solid oxide fuel cell with $La_{0.75}Sr_{0.25}CuO_{2.5-\delta}$ cathode, J. Power Sources 152 (2005) 22.
[25] T. Kato, K. Nozaki, A. Negishi, et al., J. Power Sources 133 (2004) 169.
[26] N. Grunbaum, L. Mogni, F. Prado, A. Caneiro, J. Solid State Chem. 177 (2004) 2350.